Universiteit
Leiden
The Netherlands

Quantitative pharmacology approaches to inform treatment strategies against tuberculosis

Mehta, K.

Citation
Mehta, K. (2024, May 30). *Quantitative pharmacology approaches to inform treatment strategies against tuberculosis*. Retrieved from https://hdl.handle.net/1887/3754903

Version:	Publisher's Version
License:	Licence agreement concerning inclusion of doctoral thesis in the Institutional Repository of the University of Leiden
Downloaded from:	https://hdl.handle.net/1887/3754903

Note: To cite this publication please use the final published version (if applicable).

Section III.

Quantitative Pharmacology Approaches for Newer Anti-Tuberculosis Therapeutics

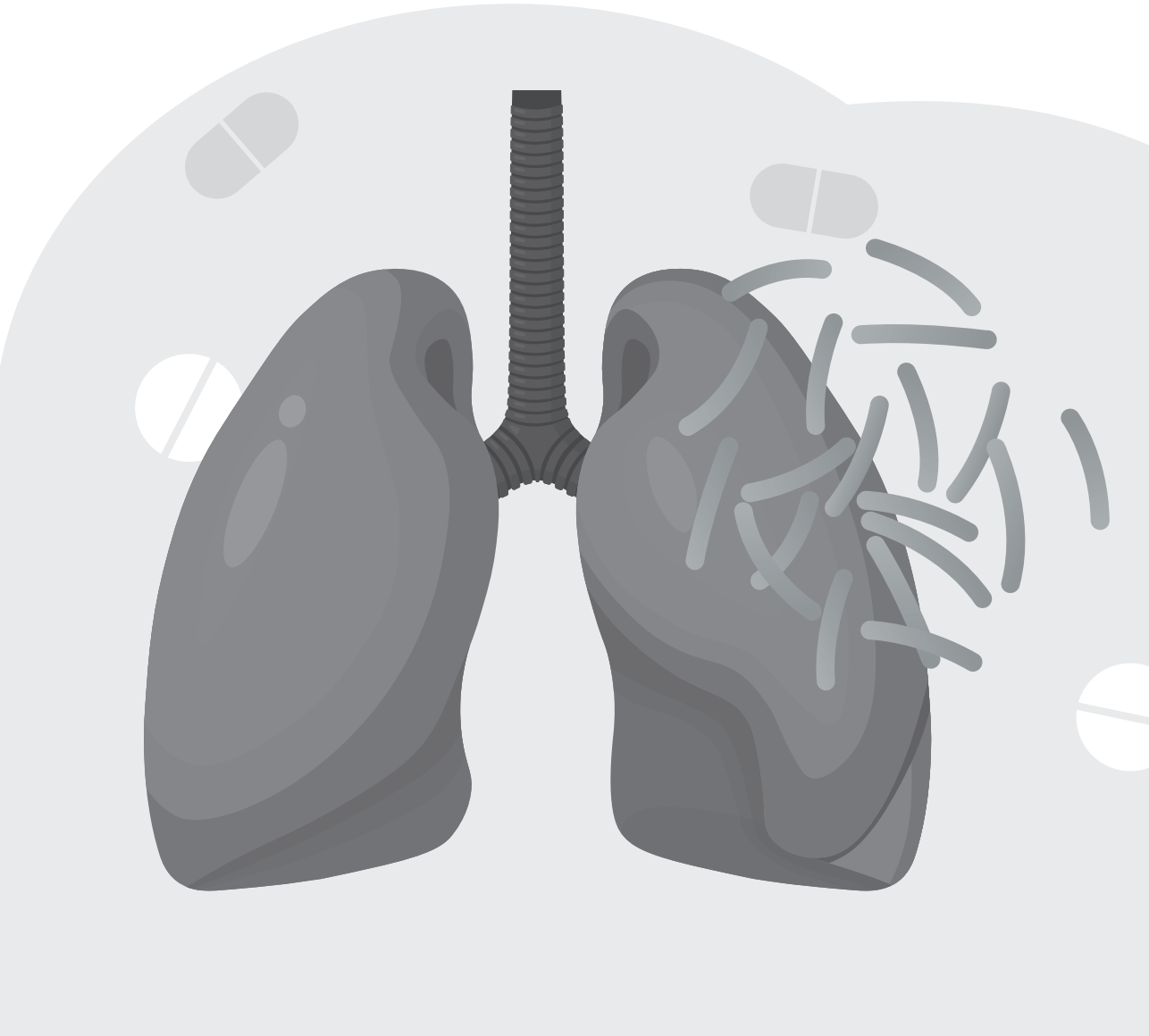

Chapter 4

Predictions of bedaquiline and pretomanid target attainment in lung lesions of tuberculosis patients using translational minimal physiologically based pharmacokinetic modeling

Krina Mehta, Tingjie Guo, Piet H van der Graaf, J G Coen van Hasselt

Clin Pharmacokinet, 2023 Mar, 62(3):519-532

Abstract

Background: Site-of-action concentrations for bedaquiline and pretomanid from tuberculosis patients are unavailable. The objective of this work was to predict bedaquiline and pretomanid site-of-action exposures using a translational minimal physiologically-based pharmacokinetic (mPBPK) approach to understand the probability of target attainment (PTA).

Methods: A general translational mPBPK framework for the prediction of lung and lung lesion exposure was developed and validated using pyrazinamide site-of-action data from mice and humans. We then implemented the framework for bedaquiline and pretomanid. Simulations were conducted to predict site-of-action exposures following standard bedaquiline and pretomanid, and bedaquiline QD dosing. Probabilities of average concentrations within lesions and lungs greater than the minimum bactericidal concentration for non-replicating (MBC_{NR}) and replicating (MBC_{R}) bacteria were calculated. Effects of patient-specific differences on target attainment were evaluated.

Results: The translational modeling approach was successful in predicting pyrazinamide lung concentrations from mice to patients. We predicted that 94% and 53% of patients would attain bedaquiline C_{avg}-lesion>MBC_{NR} during the extensive phase of bedaquiline standard (2 weeks) and QD (8 weeks) dosing, respectively. Less than 5% of patients were predicted to achieve C_{avg}-lesion>MBC_{NR} during the continuation phase of bedaquiline or pretomanid treatment. More than 80% of patients were predicted to achieve C_{avg}-lung>MBC_{R} for all simulated dosing regimens of bedaquiline and pretomanid.

Conclusions: The translational mPBPK model predicted that the standard bedaquiline continuation phase and standard pretomanid dosing may not achieve optimal exposures to eradicate non-replicating bacteria in most patients.

Introduction

Tuberculosis (TB) continues to be a global health challenge. Rifampin and isoniazid are two key first-line antibiotics against *Mycobacterium tuberculosis* (Mtb). Increasing levels and frequency of resistance against rifampin and isoniazid over time necessitated the discovery of new anti-TB antibiotics[1]. Within the last decade, two promising second-line antibiotics, bedaquiline and pretomanid, were developed as a result of increased efforts to tackle drug-resistant TB[2,3]. A combination regimen containing bedaquiline, pretomanid, and linezolid showed Mtb clearance as measured by negative culture status in 90% of patients with drug-resistant TB after 6-months of therapy[4]. BPaL is now recommended for the treatment of rifampin-resistant TB and multidrug-resistant TB patients[1].

Drug exposures at the site-of-action, within lungs, and especially within cavitary lesions, are correlated with bactericidal and sterilizing activities against Mtb. Anaerobic conditions within the necrotic region of the lesion microenvironment, caseum, provide a survival niche for nonreplicating but persistent Mtb[5]. Inadequate exposures within cavitary lesions can lead to resistance development. Measuring drug PK within the lungs and lesions of TB patients usually requires invasive methods to obtain samples and therefore is not readily possible. Preclinical animal models have traditionally been used to evaluate drug penetration at sites of action. These results require accounting for interspecies differences in physiological, pathological, and drug-specific aspects to translate to the patients[6]. Newer methods, such as, PET-imaging methods are increasingly being implemented to measure drug penetration at the site-of-action following intravenous administration of radiolabeled drugs to measure the relative fraction of drug penetration at the site-of-action[7]. A key benefit of this method is that it can be performed in the patients and as such can allow evaluations of tissue-specific PK with patient-specific covariates.

In-silico approaches allow the incorporation of available data for the development of predictive models for optimal decision-making. Population pharmacokinetics (PopPK) modeling approaches have been previously applied to quantify the relationship between plasma and lesion PK for several first-line and second-line TB antibiotics; however, this approach can only be applied when sites of action measurements are available from the patients[8,9]. Minimal physiologically-based pharmacokinetics (mPBPK) models are well suited for translational predictions of the relationship between drugs' PK in blood plasma and at sites of action and. Such models can account for known species-related differences and incorporate patient covariates and expected interindividual variability and uncertainty in the

parameter estimate to allow population simulations. The probability of target attainment (PTA) can then be predicted by defining target attainment to the desired breakpoint based on experimental data[5]. In general, several experimental methods exist to understand drug exposures at site-of-action. These methods should be used in combination with in-silico approaches to rationally predict overall treatment response in the TB patients.

Bedaquiline and its primary metabolite M2 exposures at the current standard dosing regimen (400 mg once daily (QD) for 14 days followed by 200 mg three times a week) have the potential for safety concerns related to QTc interval prolongation and hepatic adverse events[10–12]. Alternative QD dosing (200 mg QD for 8 weeks followed by 100 mg QD) of bedaquiline is of interest to increase patient adherence to obtain optimal efficacy[12]. Pretomanid has overall acceptable clinical safety profiles; however, pretomanid combination with bedaquiline and linezolid can have additive effects leading to an increased potential of certain adverse effects[13]. As such, understanding drug exposures within the systemic circulation and at sites of action is crucial to evaluate combination treatment strategies to ensure the attainment of adequate exposures to maximize efficacy, avoid resistance development, and minimize safety issues.

The main objective of this work was to predict bedaquiline and pretomanid lung- and lesion- exposures in TB patients to understand the probability of target attainment and the impact of patient covariates, body weight and cavity size, on PTA. To this end, we developed and validated a translational mPBPK modeling approach that allowed to predict bedaquiline and pretomanid PK at standard and alternative QD dosing and calculation of PTA in lungs and lesions using preclinical data.

Methods

A general translational mPBPK framework including lung and lesion was first developed and was validated using available lung PK data in mice and humans for pyrazinamide. The framework was then implemented for the development and assessments of bedaquiline and pretomanid models. Simulations were conducted to predict site-of-action exposures at standard bedaquiline and pretomanid dosing, and an alternative bedaquiline dosing. Then, the simulations were compared against critical concentration estimates to evaluate the effects of body weight and cavity size on lesion PTA.

General modeling approach

mPBPK model structure

The model development for all drugs was based on a general mPBPK structural model containing central and lung compartments[14]. The mPBPK models were parameterized using species-specific physiological parameters, such as body weight, cardiac output, lung and other tissue volumes, and volume of blood in systemic circulation[15]. Drug-specific parameters, such as blood-to-plasma ratio and plasma protein binding were obtained from the literature. Other drug-specific parameter estimates, such as absorption rates, partition coefficients, and apparent clearance (CL) were estimated using the data from PK studies in mice (S4.1). Additional structural components were evaluated in a stepwise manner as suggested by the available data and prior knowledge. For instance, plasma concentrations of the primary metabolite of bedaquiline, M2, are of importance due to its relevance to safety concerns[16,17]. Therefore, mechanistic representation of metabolism of bedaquiline to M2 was described using a liver compartment represented by the well-stirred liver model. Although in vitro and mice experimental studies have demonstrated lower anti-Mtb activity of M2 compared to bedaquiline, its site-of-action exposures can be useful to evaluate its overall impact on bacterial load in TB patients using PK-PD models; therefore, M2 lungs and lesion compartments were included in the model and the relevant parameters were estimated using mice M2 lung and lesion data. Different absorption models, i.e., multiple-site absorption, transit compartment absorption model, and dose-dependent bioavailability were evaluated.

Drug uptake in lung lesions and uninvolved lungs was described using the effect compartment structural model as described previously[18]. Rates of drug transport between systemic circulation and lesions and uninvolved lungs compartments were described by blood flow rates to these compartments calculated based on the approximate lesion and total lung volumes. The volume of lesions and uninvolved lungs were calculated based on the mean total lesion volume reported in the literature for cavitary TB patients and species-specific total lung volumes[19].

$$d/dt(Ci) = ki \times (Cbld \times Ri - Ci)$$

$$ki = Qc/Vi$$

$$Vi = Vlung \times VFi$$

Here, i represents compartments, i.e., lesion or uninvolved lungs; Ci represents drug concentration in the respective compartment; Cbld is drug concentration in systemic circulation; ki is the transfer rate constant to the respective compartment; Ri is penetration ratio for the respective compartment; Qc is cardiac output;

Vlung is the total volume of lungs; VFi is the fractional volume of the respective compartment; and Vi is the volume of the respective compartment. Mean volume of lesions (VF_{le}) was assumed 0.0216 calculated based on the mean total lesion volume, approximately 14 mL, reported in the literature for cavitary TB patients[20]. VF_{ul} was calculated as 1-VF_{le}.

Translation of the mpbpk models to tb patients

The mice mPBPK models developed using mice data were scaled to TB patients considering physiological differences between the species. Physiological parameters such as cardiac output and volumes of compartments for humans were obtained from the literature[15]. Drug-specific parameter, CL, was scaled from mice to humans using a previously known allometric exponent 0.75 for CL[21]. For the absorption rate parameter, ka, plasma PK predictions using the models scaling using allometric exponent of -0.25 and models without any scaling were compared with the observed data for each drug prior to selecting whether or not to scale ka from mice to humans. The same estimated partition coefficients and penetration ratios for each drug and compartment from mice were assumed for TB patients. To simulate a standard TB population, body weights for 500 virtual patients were sampled from the body weight distribution from clinical trial data (S4.1). Cavity presence or absence was also sampled from observed distribution from the clinical trials dataset. For virtual patients with a cavity, cavity size was simulated considering normal distribution using reported mean and standard deviation of total lesion volume in cavitary TB patients[19]. Log-normally distributed IIV of 25-40% was added in the relevant parameters. To account for uncertainty in the parameter estimates, 50 trials with the estimated RSE were simulated for each of the 500 virtual patients. All parameters for both mice and humans, including variability and RSE, are presented in **Table 4.1**.

Evaluation of the modeling approach using pyrazinamide data

An external evaluation of the predictability of our overall approach was performed using pyrazinamide plasma, lungs, and lesions PK data from mice and TB patients22,23. Therefore, preclinical mice data for pyrazinamide were digitized from the literature and were used in the pyrazinamide mPBPK model development22. Next, pyrazinamide clinical studies data were compiled from the literature23 and the Platform for Aggregation of Clinical TB Studies (TB-PACTS; https://c-path.org/programs/tb-pacts/). Simulated lesion and uninvolved lungs PK profiles of pyrazinamide were compared against available observed data in TB patients23 (S4.1).

Bedaquiline and pretomanid model development and assessment

Bedaquiline and pretomanid model development was conducted using PK data from mice. PK data from plasma, liver, and lung including both lung lesions and uninvolved lungs of mice for bedaquiline and its primary metabolite M2 were extracted from literature[22,24]. Plasma PK data from mice treated with oral pretomanid were also digitized[25]. PK concentrations from PET imaging of plasma, lung lesions, and uninvolved lungs of mice that were administered a single intravenous dose of radioactive 18F-pretomanid were also digitized[26]. The PK concentrations obtained using the PET imaging were represented as relative units (i.e., % of injected dose per mL (%ID/mL)); therefore, relevant doses were set to 100% in the analysis dataset. Model development was performed using the mPBPK generic structure as described above. Evaluations of additional drug-specific components were guided by data and the parameters were estimated using a model fitting to mice data. Model development and final model selection were guided by objective function value (OFV), the goodness of fit (predictions vs. observed) plots, physiological plausibility of parameter estimates, and precision (RSE) of the estimates.

Assessment of bedaquiline and pretomanid mice to human translated models was conducted using PK data from TB patients. Individual level PK, body weight, and cavity presentation data from various clinical studies were retrieved from the TB-PACTS database. Data from relevant dose levels and clinical studies were compiled for bedaquiline and pretomanid. Simulated plasma PK profiles for bedaquiline and pretomanid in TB patients were compared against observed data to evaluate the translated mPBPK model performance in TB patients. No lesion or uninvolved lungs PK data were available from human subjects for bedaquiline or pretomanid. Local sensitivity analysis was conducted to evaluate the impact of the parameters on steady-state plasma drug exposure was examined by introducing 10% variation in the parameters one at a time and running the simulations for 50 times.

Pharmacokinetics and target attainment predictions of bedaquiline and pretomanid at the site of action

Predictions of bedaquiline and pretomanid exposures in the lesions and uninvolved lungs were performed for 500 virtual humans using the body weight and cavity volume distributions from TB patients using the final translated mPBPK models (Table 4.1). Bedaquiline simulations included currently approved oral dosing of 400 mg QD for 14 days followed by 200 mg three times a week. The alternative bedaquiline dosing regimen included in the simulations was 200 mg QD for 8 weeks followed by 100 mg QD. Pretomanid simulations included oral dosing of 200 mg QD. Plots of the predicted lesion and uninvolved lungs PK and drug exposure matrices were prepared. Next, predicted bedaquiline and pretomanid concentrations and exposures at the site-of-action following either standard or alternative bedaquiline or standard pretomanid dosing were compared against critical concentration estimates based on in vitro experiments obtained from the literature. The range for bedaquiline and pretomanid minimum inhibitory concentrations (MIC) for MDR-TB strains, minimal bactericidal concentrations for replicating bacteria (MBC_R), and minimal bactericidal concentrations for non-replicating bacteria (MBC_{NR}) were obtained from the literature (Table 4.1)[5,27.] Plots of predicted PK exposures within lesions and lungs were plotted and compared against the MDR-TB MIC range, MBC_R, and MBC_{NR} for both drugs. Attainment of target exposures in the lesions was defined as average daily PK exposure within lesions (C_{avg}-lesion) greater than MBC_{NR} to ensure bactericidal activity against persisting, non-replicating bacteria. Body weight and cavity size from the virtual patient population were binned and PTA was calculated for each bin.

Software

All analyses were conducted in R (R for Windows, v4.1, https://www.r-project.org/) using RStudio (RStudio, v1-554, www.rstudio.com/). Data management and plotting were performed using the tidyverse package. Parameter optimization and model simulations were conducted using nlmixr and RxODE packages. Final model codes are provided in the supplementary materials (S4.2).

Figure 4.1 Final Model Structures, (A) Bedaquiline, (B) Pretomanid. The mPBPK models for bedaquiline and pretomanid contain the relevant compartments, including lung and lung lesions. Blood, liver, lungs, and lung lesions are represented by their volumes and the rest of the body is lumped into tissue compartment(s). Compartments are connected with each other by blood flows. CL=plasma clearance, DoseF=dose-dependent bioavailability, Eh=hepatic extraction ratio, F1=bioavailability of depot1, ka1=absorption rate from depot1, ka2=absorption rate from depot2, Kp=partition coefficient for tissue compartments, Qh=blood flow to liver, Qle=blood flow rate to lung lesions, Qt=blood flow to tissues, QUL=blood flow rate to unaffected lungs, Rle=penetration ratio for lung lesion, RUL=penetration ratio for unaffected lungs, Vblood=volume of blood reservoir, Vliver=volume of liver, Vtissues=volume of tissue compartment.

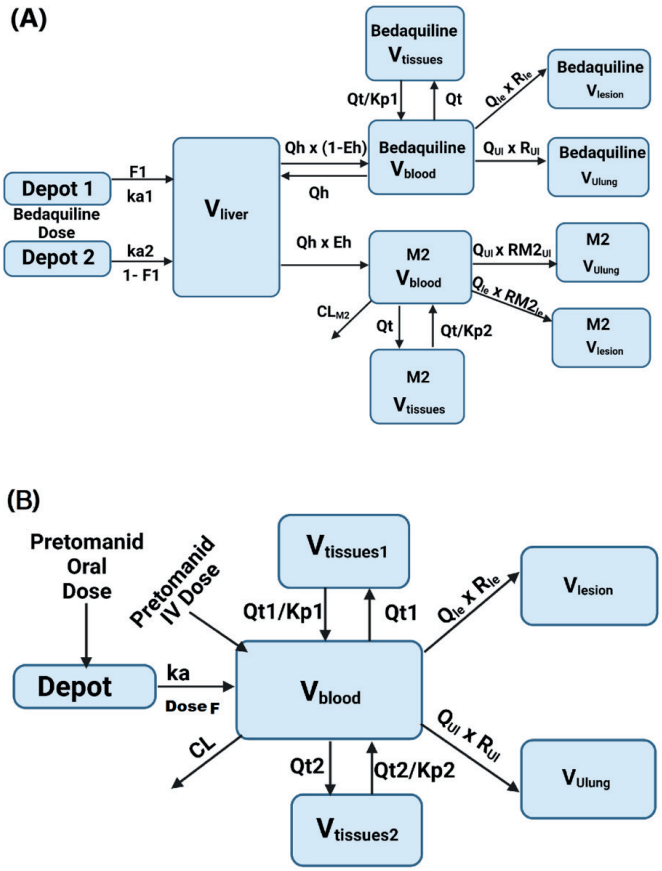

Results

Evaluation of the modeling approach using pyrazinamide data

The pyrazinamide mPBPK model was first developed using mice PK data to evaluate the predictability of our translational mPBPK approach. Pyrazinamide plasma, lung lesion, and uninvolved lungs PK data from mice were best described by the mPBPK structural model with first-order absorption and first-order elimination (S4.3). The addition of a tissue compartment and evaluations of other absorption models did not improve the model fit. The parameters describing plasma PK were estimated with good precision (RSE < 20%). The parameters R_{le} and R_{ul} were associated with an RSE of 52% and 102%, respectively (Table 4.1). The scaled mPBPK model appropriately described pyrazinamide plasma, lung lesions, and uninvolved lungs concentrations at steady-state from TB patients using allometric exponents of -0.25 for ka and 0.75 for CL **(Table 4.1, Figure 4.1)**. Overall, the pyrazinamide model predictions showed good agreement with the observed data from mice and TB patients suggesting the reliability of our translational mPBPK approach for other TB antibiotics.

Figure 4.2 Evaluation of the modeling approach using Pyrazinamide PK profiles in TB patients. Pyrazinamide model predictions showed good agreement with the observed data from TB patients suggesting the reliability of our mPBPK framework for other TB antibiotics. Pyrazinamide 1500 mg oral dosing was simulated and compared against observed data from plasma, lungs, and lesions of TB patients[23,29,39] accessed through TB-Pacts. Both observed and simulations for lung and lesion represent one dosing cycle at steady-state. Blue points=observed data, solid grey line=median of the simulations, shaded grey area=95% prediction interval (PI) of the simulations.

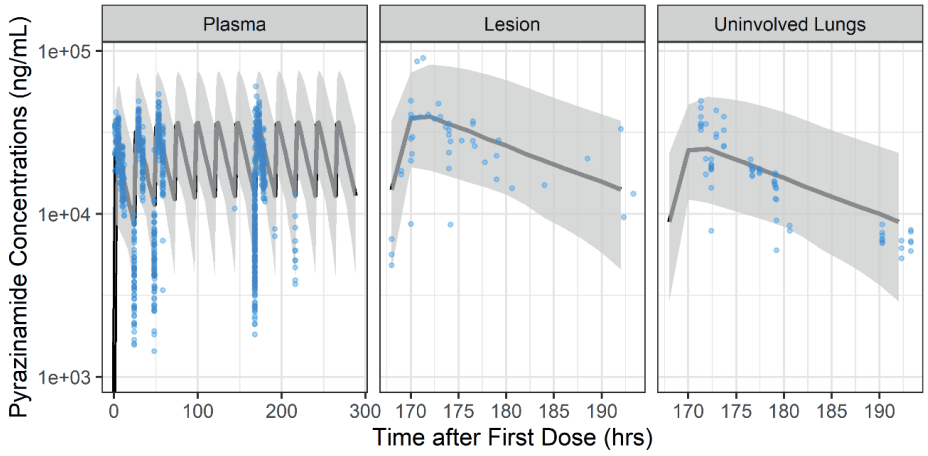

Table 4.1 Parameter estimates of Bedaquiline, Pretomanid, and Pyrazinamide mPBPK models

Parameter (Units)	Description	Parameter Estimate		%RSE	Source
		Mice	Humans		
Physiological					
Qc (L/hr)	Cardiac output	0.839	312 (for 70 kg)		15
Qh (fraction of Qc)	Blood flow to liver	0.161	0.227		
Vliv (fraction of body weight)	Volume of liver	0.0549	0.0549		
Vbl (fraction of body weight)	Volume of blood reservoir	0.077	0.077		
Bedaquiline					
fup (%)	Unbound fraction	0.1	0.1		28
BP	Blood-to-plasma ratio	1	1	-	35
ka1 (1/hr)	Absorption rate from depot1	1.3	1.3	37.8	Estimated
ka2 (1/hr)	Absorption rate from depot2	0.00501	0.00501	9.13	
CLint (L/hr)	Intrinsic clearance	1.21	60.3	16.7	
KpT	Partition coefficient for tissue compartments	4.45	4.45	15.3	
CLM2 (L/hr)	Clearance for M2	0.0119	45.9	13.6	
KpTM2	Partition coefficient for tissue compartments for M2	9.54	9.54	18.4	
R_{le}	Penetration ratio for lung lesion	11	11	10.7	
R_{ul}	Penetration ratio for uninvolved lungs	10.2	10.2	10.9	
$R_{le}M2$	Penetration ratio for lung lesion for M2	88.4	88.4	5.72	
$R_{ul}M2$	Penetration ratio for uninvolved lungs for M2	88.8	88.8	5.53	
frc	Fraction going through fast absorption (depot1)	0.609	0.609	11.9	
IIV for ka1, ka2, CLint, CLM2, KpT, and KpTM2 (%)	Lognormally distributed random variability in bedaquiline parameters for human simulations	-	40	-	
MBC_{NR}	Minimum bactericidal concentration for non-replicating bacteria (ng/mL)	-	17760	-	5
MBC_{R}	Minimum bactericidal concentration for replicating bacteria (ng/mL)	-	5500	-	5
MIC Range	Minimum inhibitory concentration range (ng/mL)	-	60-250	-	41

Parameter (Units)	Description	Parameter Estimate		%RSE	Source
		Mice	Humans		
Pretomanid					
BP	Blood-to-plasma ratio	1.65	1.65		[13]
ED50 (mg)	Dose at which bioavailability is 50% of the maximum which was assumed 1	7.59	554	14.8	Mice estimated, Humans [42]
ka (1/hr)	Absorption rate	0.3	0.3	23.3	Estimated
CL (L/hr)	Apparent clearance	0.016	4.42	3.78	
KpT	Partition coefficient for tissue compartment 1	36.3	36.3	3.77	
FT1	Fraction going to tissue compartment 1	0.97	0.97	9.72	
KpT1	Partition coefficient for tissue compartment 2	0.483	0.483	14	
R_{le}	Penetration ratio for lung lesion	1.05	1.05	145	
R_{ul}	Penetration ratio for uninvolved lungs	1.75	1.75	13.8	
IIV for ka, ED50, CL, KpT, and KpT2 (%)	Lognormally distributed random variability in pretomanid parameters for human simulations	-	40	-	
MBC_{NR}	Minimum bactericidal concentration for non-replicating bacteria (ng/mL)	-	6300	-	[13]
MBC_{R}	Minimum bactericidal concentration for replicating bacteria (ng/mL)	-	20	-	[13]
MIC Range	Minimum inhibitory concentration range (ng/mL)	-	8 - 4000	-	[13]
Pyrazinamide					
BP	Blood-to-plasma ratio	0.79	0.79	-	[43]
ka (1/hr)	Absorption rate	0.30	0.05[a]	7.25	Estimated
CL (L/hr)	Apparent clearance	0.014	3.5	3.04	
R_{le}	Penetration ratio for lung lesion	1.37	1.37	52.2	
R_{ul}	Penetration ratio for uninvolved lungs	0.85	0.85	102	
IIV for ka and CL (%)	Lognormally distributed random variability in pyrazinamide parameters for human simulations (%)	-	40	-	

[a] allometrically scaled from mice to humans using exponent -0.25; Estimated residual errors in model fitting to mice data were as following: combined bedaquiline plasma, liver, and M2 plasma = proportional 43 %; bedaquiline and M2 lesion and lungs = proportional 53%, pretomanid plasma= proportional 12 %, pretomanid lesion = proportional 6% and additive 2.24 ng/mL, pretomanid lungs = proportional 12 % and additive 0.239 ng/mL, pyrazinamide combined plasma, lungs, and lesion= proportional 35%. Residual errors were not included in the human simulations.

Model development and assessment for bedaquiline and pretomanid

Bedaquiline and M2 PK data from plasma, liver, lung lesions, and uninvolved lungs of Mtb infected mice was best described by the mPBPK structural model containing parallel first-order two absorptions that are in alignment with prior bedaquiline PopPK models, parent-metabolite well-stirred liver compartment, tissue compartments for both bedaquiline and M2, first-order elimination of M2, and lung lesion and uninvolved lungs compartments **(Figure 4.1A)**. Other components that were evaluated but did not provide improvements in the model fit included only one first-order absorption, transit compartment absorption, and saturable conversion of bedaquiline to M2. All parameters were estimated with reasonable precision (RSE < 40%) **(Table 4.1)**, and the model predictions showed good agreement with the observed data in mice **(Figure 4.3A,** S4.4A**)**.

Slight under-predictions of bedaquiline and over-predictions of M2 plasma concentrations were noted when the mPBPK model was directly scaled from mice to humans using only allometric scaling. This was assumed to be due to the species difference between mice and humans in bedaquiline and M2 metabolism and has been previously noted[24,28]. To account for this difference, calibration of two parameters, intrinsic clearance (CLint) and clearance of M2 (CLM2) was performed by fitting to median rich concentrations-time profiles from TB patients for one dose group (400 mg on day1, 300 mg on day2, and 200 mg day3-14)[29]. The updated model predicted both bedaquiline and M2 plasma concentrations time profiles well for all dose groups in the dataset **(Table 4.2, Figure 4.4)**. With a 10% or 50% variation in parameter estimates, the mean sensitivity index was low (between -1 and 1) for both bedaquiline and M2 with the exception of absorption rate of depot2 (ka2) that showed high sensitivity for both bedaquiline and M2 plasma concentrations (S4.6). Overall, this mPBPK model for bedaquiline and M2 was deemed reliable for predictions of exposures at the site-of-action, within lung lesions, in TB patients.

Pretomanid oral absorption was best described by a first-order absorption model with dose-dependent bioavailability. Transit compartment absorption was evaluated but did not provide improvements in the model fits. Pretomanid plasma PK after oral dosing, and F18-pretomanid plasma, lung lesion, and uninvolved lungs PK after F18-pretomanid IV dosing were best described by the mPBPK structural model with two tissue compartments and first-order elimination **(Figure 4.2B)**. All parameters were estimated with reasonable precision (RSE < 45%) except that R_{le} was estimated with RSE of 145% due to limited lesion PK data **(Table 4.1)**. Overall, the model predictions showed good agreement with the observed data

from mice following either F18-pretomanid IV or pretomanid oral dosing **(Figure 4.3B)**. Reasonable agreement between observed data and scaled-up human model predictions was noticed for plasma PK data for pretomanid from TB patients, although some underpredictions were noted at 1000 mg and 1200 mg doses **(Table 4.2, Figure 4.4)**. With a 10% change in parameter estimates, the sensitivity for key pretomanid PK parameters was relatively low (between -2.5 and 2.5) with the exception of partition coefficient for tissue compartment 1 (kpT1) that showed moderate sensitivity for pretomanid plasma concentrations. This further supported the reliability of the model (S4.6). Overall, the mPBPK model for pretomanid was deemed reliable for predictions of exposures at the site-of-action, within lung lesions, following clinically-relevant doses in TB patients.

Figure 4.3 Predicted vs. observed PK profiles in mice, (A) Bedaquiline, (B) Pretomanid. The model predictions for plasma, lung, and lesion bedaquiline and pretomanid agreed well with the observed data for mice. Bedaquiline 25 mg/kg was administered orally[22]. Pretomanid was administered orally at varying doses between 18 mg/kg to 486 mg/kg[25,26]. Radioactive 18F pretomanid was administered intravenously and the % of the injected dose was measured in plasma, lungs, and lesions of mice. Blue points=observed data, black line=model fit predictions, %ID= percent of injected dose, pretomanid concentrations for oral dosing unit=ng/mL, 18F-pretomanid concentrations for IV dosing=%ID/mL.

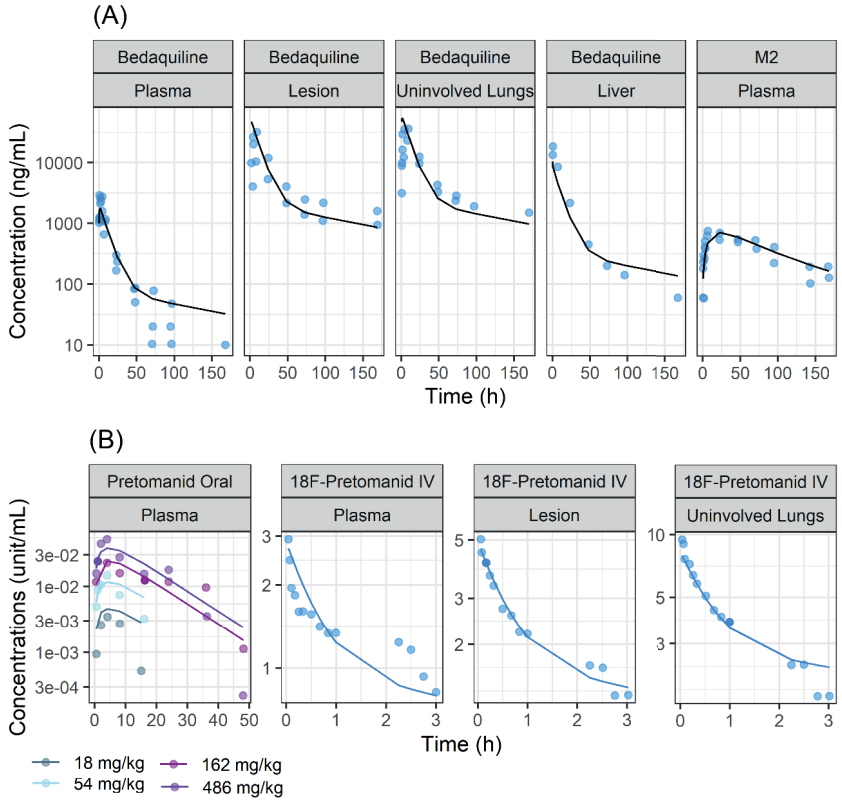

Figure 4.4 Predicted and observed plasma PK profiles in TB patients for Bedaquiline, M2, and Pretomanid. The model predictions for plasma bedaquiline, M2, and pretomanid agreed well with the observed data for TB patients from clinical trials at various doses[29,40]. Blue points=observed data, solid grey line=median of the simulations, shaded grey area=95% prediction interval (PI) of the simulations. Panel titles represent bedaquiline or pretomanid doses in mg. Bedaquiline was administered as an increasing daily dose, i.e., panel 1 represents a group that received 200 mg on day1 and 100 mg on day2 onwards.

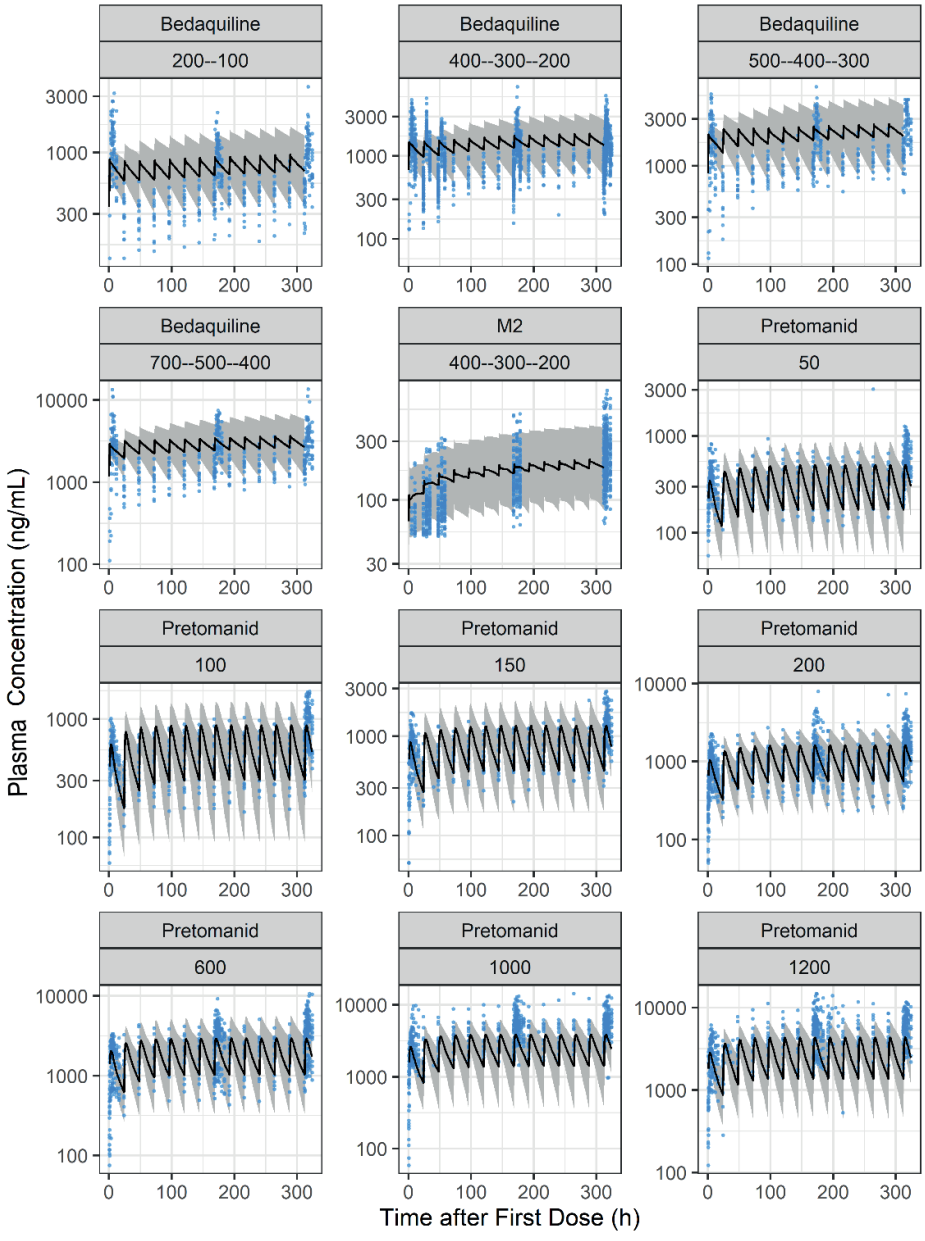

Pharmacokinetics and target attainment predictions of bedaquiline and pretomanid at the site of action

The simulations suggested good penetration for both bedaquiline in lung lesions and uninvolved lungs **(Figure 4.5A)**. The predicted bedaquiline median (95% prediction interval) lesion-to-plasma ratio was 11.0 (10.5-11.4) and uninvolved-lungs-to-plasma was 10.2 (9.8-10.5). Bedaquiline lesions and uninvolved lungs concentrations were predicted to remain above the MIC range observed for MDR-TB isolates at standard dosing and alternative QD dosing[27]. Bedaquiline lesion and uninvolved lungs concentrations were predicted to be slightly above MBC_R for all virtual patients throughout the treatment period during extensive phase of standard dosing and alternative QD dosing **(Figure 4.5A)**[5,27]. At standard bedaquiline dosing, a total of 94% of virtual patients were predicted to have Cavg-lesion > MBC_{NR} after extensive dosing (400 mg QD) for the first 14 days of treatment, but <5% of virtual patients were predicted to have Cavg-lesion > MBC_{NR} throughout the continuation phase of treatment when dosing was reduced to 200 mg three times a week. At alternative QD bedaquiline dosing, a total of 86% of virtual patients were predicted to have Cavg-lesion > MBC_{NR} during extensive phase (200 mg QD) for the 8 weeks of treatment, but <5% of virtual patients were predicted to have Cavg-lesion > MBC_{NR} throughout the continuation phase of treatment when dosing was reduced to 100 mg QD. The simulations also suggested relatively similar M2 exposures at site-of-action to those of bedaquiline **(Figure 4.5)**. Simulated plasma M2 concentrations were below reported M2 EC50 concentrations for QTcF prolongation for 83% of virtual patients during extensive phase of standard bedaquiline treatment, and for all virtual patients during continuation phase of standard bedaquiline and both phases of alternative QD dosing (S4.4B). It should be noted that although the probability of target attainment is higher with bedaquiline standard dosing during the extensive phase, the period of extensive phase in standard dosing vs. alternative QD dosing is shorter (2 vs. 8 weeks) which may have a large impact on overall efficacy. The probability of Cavg-lesion >MBC_{NR} was predicted to increase with an increase in body weight for both dosing scenarios **(Figure 4.6)**. Cavity size was predicted to not affect the attainment of average lesion concentrations above MBC_{NR}.

Pretomanid predicted median (95% prediction interval) lesion-to-plasma ratio was 2.6 (2.5-2.8) and uninvolved-lung-to-plasma ratio was 2.9 (2.7-3.1) (Figure 4.5B). Predicted lesion concentrations after pretomanid 200 mg daily dosing were predicted to remain above the pretomanid MIC range observed for MDR-TB isolates for 18% of virtual patients[13]. Pretomanid lesions and uninvolved lungs concentrations were predicted to remain well above (MBC_R) for all patients. Less than 1% of patients were predicted to have pretomanid Cavg-lesion> MBC_{NR} **(Figure 4.5B)**[13].

Table 4.2 Observed vs. predicted exposure comparison for Bedaquiline and Pretomanid at standard dosing at steady-state.

Exposure Metric (mg/L)	Bedaquiline 400 mg QD		Bedaquiline 200 mg Thrice a Week		Pretomanid 200 mg QD	
	Observed [28]	Predicted	Observed [28]	Predicted	Observed [13]	Predicted
$Cavg_{ss}$	2.696 (0.865) [a] 1.371 (0.529) [b]	3.24 (0.497)	0.584 (0.197)	0.68 (0.108)	1.26 (0.16)	1.06 (0.143)
$Cmax_{ss}$	5.502 (2.965) [a] 2.763 (1.185) [b]	6.29 (1.45)	1.267 (0.435)	1.57 (0.404)	1.7 (0.29)	3.06 (0.61)
$Cmin_{ss}$	1.448 (0.437) [a] 0.728 (0.257) [b]	1.07 (0.322)	0.356 (0.170)	0.174 (0.062)	0.5 (0.08)	0.149 (0.06)

[a] Drug-susceptible TB patients, [b] MDR-TB patients. All values are presented as mean (standard deviation)

Figure 4.5 Simulated PK profiles at sites of action in TB patients: (A) Bedaquiline standard and QD dosing, and (B) Pretomanid. Bedaquiline standard dosing included 400 mg QD for 14 days followed by 200 mg three days a week. Bedaquiline QD dosing included 200 mg QD for 8 weeks followed by 100 mg QD. Pretomanid dosing included 200 mg QD. The model predicted that lung and lesion concentrations of bedaquiline and pretomanid would remain above MIC (for rifampin and/or isoniazid drug-resistant TB strains) and MBCR at current clinically-relevant doses. Although it was predicted that 94% and 53% of patients would achieve target exposures at standard and alternative QD bedaquiline dosing, respectively; it should be noted that alternative QD dosing provides higher target attainment for a longer duration (2 vs. 8 weeks). M2 target attainment was predicted to be slightly higher than those of bedaquiline. It should be noted that M2 MBC and MICs were assumed the same as those of bedaquiline[41]. MIC= minimum inhibitory concentrations, MDR= multi-drug resistant tuberculosis, MBCR = minimum bactericidal concentrations for replicating bacteria, MBCNR = minimum bactericidal concentrations for non-replicating bacteria. Blue or black lines=median of the simulations, shaded blue or grey area=95% prediction interval (PI) of the simulations.

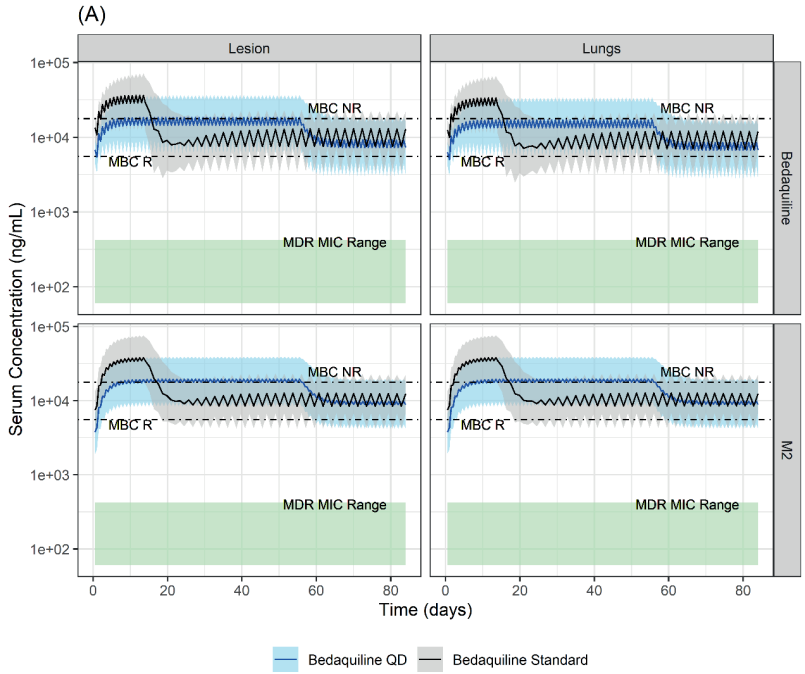

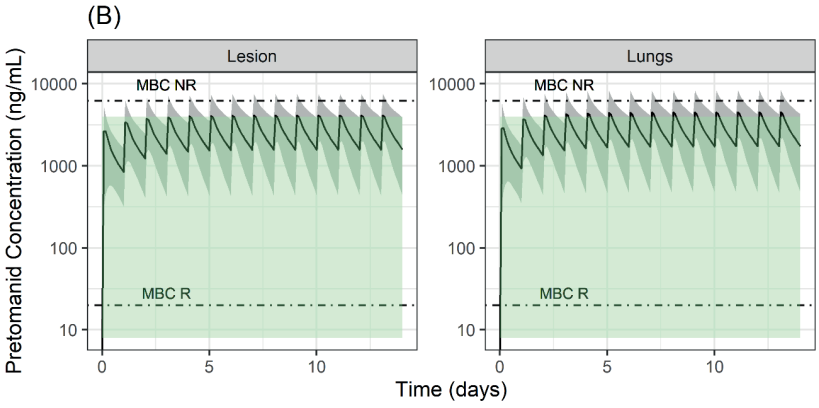

Figure 4.6 Predicted probability of average Bedaquiline concentrations above MBCNR in TB patients by body weight. Body weight was predicted to have an impact on lesion PTA. PTA was defined as Cavg-lesion > MBC NR. MBCNR = minimum bactericidal concentrations for non-replicating bacteria. PTA were calculated at steady-state for each dosing group.

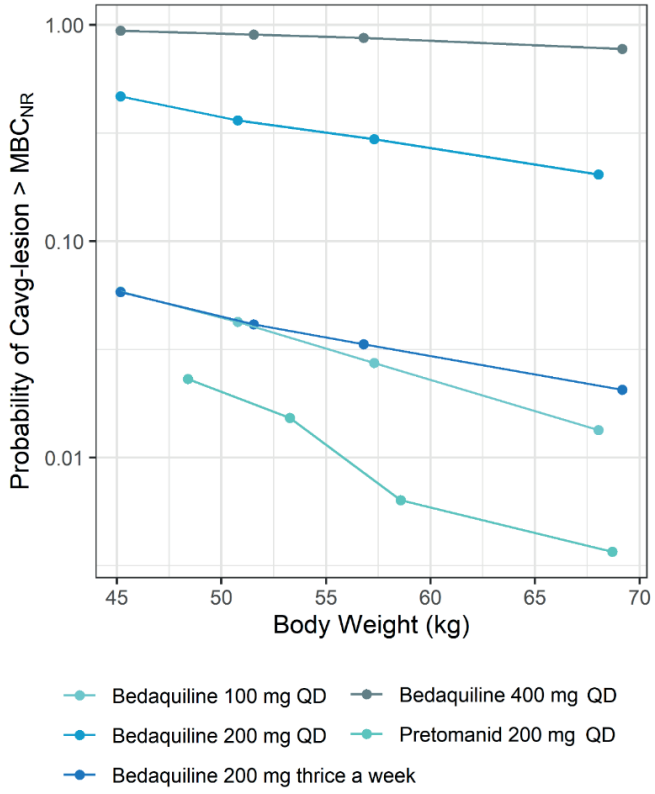

Discussion

In this work, we developed translational mPBPK models for bedaquiline and pretomanid containing lungs including cavitary lesions compartments using physiological parameters describing blood flows and volumes of lesions and uninvolved lungs. The mPBPK models adequately described plasma, lungs, and lesion PK data from mice well. The translational mPBPK models adequately described dose-ranging plasma PK data from TB patients. The mPBPK models allowed predictions of bedaquiline and pretomanid exposures and target attainment in the lungs and lesions of TB patients.

One of the concerns against the newer antibiotics, bedaquiline and pretomanid, is the development of resistance[30]. A key mechanism of resistance development against antibiotics includes a subpopulation of Mtb, persisters, developing phenotypic tolerance against the drugs without genetic mutations. This process is reversible; however, sub-optimal drug exposures within cavitary lesions where persisters dwell, allow them to survive. This eventually allows Mtb strains to develop genotypic mutation and allow replication of genetically resistant strains against antibiotics[31]. As such, it is crucial to optimize therapeutic strategies to eliminate the non-replicating persistent Mtb population during the treatment phase. Our mPBPK models can be combined with various types of experimental in vitro and in vivo bacterial-kill dynamics and resistance development data to construct mechanistic PK-PD models that can be used to further evaluate optimal strategies against Mtb, especially against persisters within lesions[32].

Our predictions suggested that PTA decrease with an increase in patients' body weight for both bedaquiline and pretomanid. The current dosing regimen for bedaquiline is associated with safety risks of QTcF prolongation and hepatic adverse events; therefore, an increase in bedaquiline dosing may not be a viable approach for all patients. Further efficacy and safety evaluations of bodyweight-based dose optimization for bedaquiline may be useful. The model also captured the pharmacokinetics of the bedaquiline metabolite M2 within plasma and at site-of-action. To further evaluate the contribution of M2 on Mtb clearance using the developed mPBPK framework, M2-specific pharmacodynamic parameters such as derived in an in vitro experiment would be required. Model-informed precision dosing approaches can be employed to ensure maximum risk-benefit balance for most patients considering totality of information[33,34]. The current dosing regimen for pretomanid is considered safe. The mechanistic PK-PD model can be used

to predict the effects of alternative dosing of pretomanid in combination with bedaquiline and/or other antibiotics on clearance of persisting Mtb from lesion.

Previously, standard compartmental models combined with effect compartment structural models or whole-body PBPK modeling combined with mechanistic lung models have been developed for mostly first-line TB antibiotic[8,9,35]. Middle-out approaches, such as mPBPK models, allow the balance between empirical compartmental models and rigorous whole-body PBPK models[36]. Our mPBPK model construct included standard physiological parameters, such as blood flow rates and volume for lungs. A key component of our structural model is the parameter describing flow rates to lesions that were calculated based on total blood flow rates and volume fraction of cavitary lesion. As such, this approach suggests a simple technique to evaluate the impact of cavitary lesion size on target exposure attainment within lesions for anti-TB agents. Our simulations suggested no significant impact of total lesion volume on PTA within lesions for bedaquiline and pretomanid given other variability and uncertainty in the parameters that were estimated using limited preclinical data. Additional model-based analyses using our structural model and longitudinal PET-imaging data from lesions of varying sizes from TB patients[7] may allow further insights into understating the impact of cavity size on bedaquiline and pretomanid target attainment within lesions to further optimize treatment strategies.

In vitro experimental evaluations of MIC and MBC values for antimicrobials are usually performed using free drug. As such, the role of plasma protein binding may be important for in vitro – in vivo response comparisons if plasma drug concentrations are used for predictions of response in vivo. Generally, only unbound drug from the systemic circulation is available for diffusion into the tissues. Both bound and unbound drug can penetrate the tissues via active transport; however, as distribution equilibrium is achieved, unbound plasma and unbound tissue concentrations reach equilibrium[37,38]. The previously described empirical model structure for tissue penetration that was fitted to the observed lung and lesion concentrations data allows estimation of lung and lesion distribution parameters relative to plasma drug concentrations, and may empirically account for the contributions of the plasma protein binding[8,18]. Following drug penetration to the lung tissue, the fraction of drug available to exert the effect depends on the tissue content and drug physicochemical properties, such as lipophilicity, solubility, tissue protein binding, and acidity[37,38]. Therefore, accounting for fraction unbound in tissue for predictions of PK-PD relationship may be important[5]. In this work, we did not directly correct site of action exposures for protein or tissue binding process

as uncertainty exists in the overall impact of these parameters on the PK-PD relationship for bedaquiline and pretomanid. Evaluations of these relationships may be of interest in future studies.

Our mPBPK models were calibrated to mice PK data. The models were translated to TB patients using allometric scaling and were compared and qualified against dose-ranging plasma concentrations data from clinical studies. Although our translational models provided reasonable agreement with the observed plasma concentrations data for all three drugs, this work did not include evaluations of best structural model fit to the clinical data or estimation of individual parameter estimation. The sensitivity analysis identified the most sensitive parameters. The future work may consider estimation of individual parameters using the mPBPK model structure, including further evaluations of the role of the sensitive parameters on exposure using clinical data. Mechanistic understanding included in the mPBPK construct combined with Bayesian estimation using our final parameter estimates as priors may provide thorough understanding of individual variability and covariate-parameter relationships towards the goal of treatment optimization, especially against persisting Mtb.

Although the validation of our translational approach for predictions of lesion and lung concentrations using pyrazinamide give confidence in the applied approach, our model predictions for lesion and lung concentrations for bedaquiline and pretomanid cannot be compared to observed data from TB patients as such data are not available to date. Our models may be further validated or further developed in the future when such data is available. In general, the current construct of mPBPK models for bedaquiline and pretomanid are relevant for our primary objective, i.e., to predict exposures in the lungs and lesions of TB patients using preclinical data. Additionally, the good performance of our translational mPBPK approach for pyrazinamide gives confidence that similar translational performance may be expected for other drugs, such as, bedaquiline and pretomanid.

To conclude, we present the first translational mPBPK models for bedaquiline and pretomanid allowing comprehensive predictions of lungs and lesions exposures in patients. Both extensive and continuation phase of current standard bedaquiline dosing were predicted to achieve target exposures within lungs and cavitary lesions to elicit bactericidal activity against replicating bacteria; however, only extensive phase treatment was predicted to achieve target exposures to elicit minimum bactericidal activity against non-replicating bacteria. Standard pretomanid dosing was predicted to achieve target exposures to elicit bactericidal

activity against replicating bacteria but not against non-replicating bacteria for most patients. These models can also be further developed to be combined with pharmacodynamics, efficacy, or safety measures to optimize or individualize combination treatment strategies.

References

1. World Health Organization. Consolidated Operational Guidelines on Handbook Tuberculosis. 2020. 132 p.
2. Khoshnood S, Goudarzi M, Taki E, Darbandi A, Kouhsari E, Heidary M, et al. Bedaquiline: Current status and future perspectives. J Glob Antimicrob Resist [Internet]. 2021;25:48–59. Available from: https://doi.org/10.1016/j.jgar.2021.02.017
3. Stancil SL, Mirzayev F, Abdel-Rahman SM. Profiling pretomanid as a therapeutic option for tb infection: Evidence to date. Drug Des Devel Ther. 2021;15:2815–30.
4. Conradie F, Diacon AH, Ngubane N, Howell P, Everitt D, Crook AM, et al. Treatment of Highly Drug-Resistant Pulmonary Tuberculosis. N Engl J Med. 2020;382(10):893–902.
5. Sarathy JP. Caseum : a Niche for Mycobacterium tuberculosis Drug-Tolerant.
6. Ernest JP, Strydom N, Wang Q, Zhang N, Nuermberger E, Dartois V, et al. Development of New Tuberculosis Drugs: Translation to Regimen Composition for Drug-Sensitive and Multidrug-Resistant Tuberculosis. Annu Rev Pharmacol Toxicol. 2021;61:495–516.
7. Ordonez AA, Wang H, Magombedze G, Ruiz-CA, Srivastava S, Chen A, et al. Heterogeneous Drug Exposures in Pulmonary Lesions. HHS Public Access. 2020;26(4):529–34.
8. Kjellsson MC, Via LE, Goh A, Weiner D, Low KM, Kern S, et al. Pharmacokinetic evaluation of the penetration of antituberculosis agents in rabbit pulmonary lesions. Antimicrob Agents Chemother. 2012 Jan;56(1):446–57.
9. Strydom N, Gupta S V., Fox WS, Via LE, Bang H, Lee M, et al. Tuberculosis drugs' distribution and emergence of resistance in patient's lung lesions: A mechanistic model and tool for regimen and dose optimization. Vol. 16, PLoS Medicine. 2019.
10. Dooley KE, Rosenkranz SL, Conradie F, Moran L, Hafner R, von Groote-Bidlingmaier F, et al. QT effects of bedaquiline, delamanid, or both in patients with rifampicin-resistant tuberculosis: a phase 2, open-label, randomised, controlled trial. Lancet Infect Dis [Internet]. 2021 Jul 1;21(7):975–83. Available from: https://doi.org/10.1016/S1473-3099(20)30770-2
11. Cohen K, Maartens G. A safety evaluation of bedaquiline for the treatment of multi-drug resistant tuberculosis. Expert Opin Drug Saf [Internet]. 2019;18(10):875–82. Available from: https://doi.org/10.1080/14740338.2019.1648429
12. Tanneau L, Karlsson MO, Rosenkranz SL, Cramer YS, Shenje J, Upton CM, et al. Assessing Prolongation of the Corrected QT Interval with Bedaquiline and Delamanid Coadministration to Predict the Cardiac Safety of Simplified Dosing Regimens. Clin Pharmacol Ther. 2022;0(0):1–9.
13. FDA, Center For Drug Evaluation and Research. Center for Drug Evaluation and Research Application Number: 211810Orig1s000: MULTI-DISCIPLINE REVIEW. 2016;1–264. Available from: https://www.accessdata.fda.gov/drugsatfda_docs/nda/2019/212862Orig1s000MultidisciplineR.pdf
14. Jermain B, Hanafin PO, Cao Y, Lifschitz A, Lanusse C, Rao GG. Development of a Minimal Physiologically-Based Pharmacokinetic Model to Simulate Lung Exposure in Humans Following Oral Administration of Ivermectin for COVID-19 Drug Repurposing. J Pharm Sci. 2020 Dec;109(12):3574–8.
15. Brown RP, Delp MD, Lindstedt SL, Rhomberg LR, Beliles RP. Physiological parameter values for physiologically based pharmacokinetic models. Toxicol Ind Health. 1997;13(4):407–84.
16. Ngwalero P, Brust JCM, van Beek SW, Wasserman S, Maartens G, Meintjes G, et al. Relationship between plasma and intracellular concentrations of bedaquiline and its m2 metabolite in South African patients with rifampin-resistant tuberculosis. Antimicrob Agents Chemother. 2021;65(11).
17. Tanneau L, Svensson EM, Rossenu S, Karlsson MO. Exposure–safety analysis of QTc interval and transaminase levels following bedaquiline administration in patients with drug-resistant tuberculosis. CPT Pharmacometrics Syst Pharmacol. 2021;10(12):1538–49.
18. Gobburu JVS, Tammara V, Lesko L, Jhee SS, Sramek JJ, Cutler NR, et al. Pharmacokinetic-pharmacodynamic modeling of rivastigmine, a cholinesterase inhibitor, in patients with Alzheimer's disease. J Clin Pharmacol [Internet]. 2001 Oct 1;41(10):1082–90. Available from: https://doi.org/10.1177/00912700122012689

19. Chen RY, Yu X, Smith B, Liu X, Gao J, Diacon AH, et al. Radiological and functional evidence of the bronchial spread of tuberculosis: an observational analysis. The Lancet Microbe [Internet]. 2021;2(10):e518–26. Available from: http://dx.doi.org/10.1016/S2666-5247(21)00058-6

20. Chen RY, Yu X, Smith B, Liu X, Gao J, Diacon AH, et al. Radiological and functional evidence of the bronchial spread of tuberculosis: an observational analysis. The Lancet Microbe. 2021 Oct;2(10):e518–26.

21. Mahmood I, Balian JD. The Pharmacokinetic Principles Behind Scaling from Preclinical Results to Phase I Protocols. Clin Pharmacokinet [Internet]. 1999;36(1):1–11. Available from: https://doi.org/10.2165/00003088-199936010-00001

22. Irwin SM, Prideaux B, Lyon ER, Zimmerman MD, Brooks EJ, Schrupp CA, et al. Bedaquiline and Pyrazinamide Treatment Responses Are Affected by Pulmonary Lesion Heterogeneity in Mycobacterium tuberculosis Infected C3HeB/FeJ Mice. ACS Infect Dis. 2016;2(4):251–67.

23. Prideaux B, Via LE, Zimmerman MD, Eum S, Sarathy J, O'Brien P, et al. The association between sterilizing activity and drug distribution into tuberculosis lesions. Nat Med. 2015;21(10):1223–7.

24. Rouan MC, Lounis N, Gevers T, Dillen L, Gilissen R, Raoof A, et al. Pharmacokinetics and pharmacodynamics of TMC207 and its N-desmethyl metabolite in a murine model of tuberculosis. Antimicrob Agents Chemother. 2012;56(3):1444–51.

25. Ahmad Z, Peloquin CA, Singh RP, Derendorf H, Tyagi S, Ginsberg A, et al. PA-824 exhibits time-dependent activity in a murine model of tuberculosis. Antimicrob Agents Chemother. 2011;55(1):239–45.

26. Filipa Mota, PhD, Camilo Ruiz-Bedoya, MD, Elizabeth Tucker, MD, Patricia De Jesus, BS, Kelly Flavahan, Mitchell Turner, BA, Clara Erice, PhD, Melissa Bahr, BA, John Kim, BA, Farina Mahmud, PhD, Charles A Peloquin, Pharm.D, Charles A Peloquin, Pharm.D, Alvaro A Ordonez, MD, Sanjay K Jain, MD, Sanjay K Jain, MD, 1411. Noninvasive Assessment of Intralesional Antimicrobial Concentration-Time Profiles in Pulmonary and Central Nervous System Tuberculosis using Dynamic 18F-Pretomanid Positron Emission Tomography, Open Forum Infectious Diseases, Volume 8, Issue Supplement_1, November 2021, Pages S789–S790, https://doi.org/10.1093/ofid/ofab466.1603

27. Ismail NA, Omar S V., Joseph L, Govender N, Blows L, Ismail F, et al. Defining Bedaquiline Susceptibility, Resistance, Cross-Resistance and Associated Genetic Determinants: A Retrospective Cohort Study. EBioMedicine [Internet]. 2018;28:136–42. Available from: https://doi.org/10.1016/j.ebiom.2018.01.005

28. van Heeswijk RPG, Dannemann B, Hoetelmans RMW. Bedaquiline: A review of human pharmacokinetics and drug-drug interactions. J Antimicrob Chemother. 2014;69(9):2310–8.

29. Diacon AH, Dawson R, Von Groote-Bidlingmaier F, Symons G, Venter A, Donald PR, et al. Bactericidal activity of pyrazinamide and clofazimine alone and in combinations with pretomanid and bedaquiline. Am J Respir Crit Care Med. 2015;191(8):943–53.

30. Chesov E, Chesov D, Maurer FP, Andres S, Utpatel C, Barilar I, et al. Emergence of bedaquiline resistance in a high tuberculosis burden country. Eur Respir J [Internet]. 2022;59(3):1–10. Available from: http://dx.doi.org/10.1183/13993003.00621-2021

31. Allué-Guardia A, Garcia-Vilanova A, Olmo-Fontánez AM, Peters J, Maselli DJ, Wang Y, et al. Host- and Age-Dependent Transcriptional Changes in Mycobacterium tuberculosis Cell Envelope Biosynthesis Genes after Exposure to Human Alveolar Lining Fluid. Int J Mol Sci [Internet]. 2022;23(2). Available from: https://www.mdpi.com/1422-0067/23/2/983

32. Drusano GL, Kim S, Almoslem M, Schmidt S, D'Argenio DZ, Myrick J, et al. The funnel: A screening technique for identifying optimal two-drug combination chemotherapy regimens. Antimicrob Agents Chemother. 2021;65(2).

33. Jarugula P, Scott S, Ivaturi V, Noack A, Moffett BS, Bhutta A, et al. Understanding the Role of Pharmacometrics-Based Clinical Decision Support Systems in Pediatric Patient Management: A Case Study Using Lyv Software. J Clin Pharmacol. 2021 Jun;61 Suppl 1:S125–32.

34. Hughes JH, Tong DMH, Lucas SS, Faldasz JD, Goswami S, Keizer RJ. Continuous Learning in Model-Informed Precision Dosing: A Case Study in Pediatric Dosing of Vancomycin. Clin Pharmacol Ther. 2021;109(1):233–42.

35. Humphries H, Almond L, Berg A, Gardner I, Hatley O, Pan X, et al. Development of physiologically-based pharmacokinetic models for standard of care and newer tuberculosis drugs. CPT Pharmacometrics Syst Pharmacol. 2021;10(11):1382–95.

36. Cao Y, Jusko WJ. Applications of minimal physiologically-based pharmacokinetic models. J Pharmacokinet Pharmacodyn. 2012;39(6):711–23.

37. Rowland M, Tozer TN. Clinical Pharmacokinetics and Pharmacodynamics: Concepts and Applications. In 1980.

38. Shargel L, Wu-Pong S, Yu ABC. Chapter 10. Physiologic Drug Distribution and Protein Binding. In: Applied Biopharmaceutics & Pharmacokinetics, 6e [Internet]. New York, NY: The McGraw-Hill Companies; 2012. Available from: http://accesspharmacy.mhmedical.com/content.aspx?aid=56603200

39. Diacon AH, Dawson R, von Groote-Bidlingmaier F, Symons G, Venter A, Donald PR, et al. 14-day bactericidal activity of PA-824, bedaquiline, pyrazinamide, and moxifloxacin combinations: a randomised trial. Lancet [Internet]. 2012 Sep 15;380(9846):986–93. Available from: https://doi.org/10.1016/S0140-6736(12)61080-0

40. The global alliance for tb drug development. Evaluation of Early Bactericidal Activity in Pulmonary Tuberculosis (TMC207-CL001). https://clinicaltrials.gov/show/NCT01215110. 2017.

41. Kim S, Yamada WM, Duncanson B, Nole J, Rogers S, Parker S, et al. Building Optimal Three-Drug Combination Chemotherapy Regimens To Eradicate Mycobacterium tuberculosis in Its Slow-Growth Acid Phase. Antimicrob Agents Chemotherapy. 2021;65(10):e00693-21. Available from: https://journals.asm.org/doi/abs/10.1128/AAC.00693-21

42. Lyons MA. Pretomanid dose selection for pulmonary tuberculosis: An application of multi-objective optimization to dosage regimen design. CPT Pharmacometrics Syst Pharmacol. 2021;10(3):211–9.

43. Muliaditan M, Della Pasqua O. Evaluation of pharmacokinetic-pharmacodynamic relationships and selection of drug combinations for tuberculosis. Br J Clin Pharmacol. 2021 Jan;87(1):140–51.

Supplementary Materials

S4.1. Summary of the time course data used for model development and validation

Drug Name	Study Details	Source
Model Development		
Bedaquiline	Bedaquiline concentrations from blood plasma and liver of mice after a single oral dose of 25 mg/kg bedaquiline	[1]
	Bedaquiline and M2 concentrations from blood plasma, lesion, and uninvolved lungs of mice after a single oral dose of 25 mg/kg bedaquiline	[2]
Pretomanid	Pretomanid concentrations from blood serum of mice after single oral doses of either 6-, 18-, 54-, 162-, or 486- mg/kg pretomanid	[3]
	F18-pretomanid plasma, lesion, and uninvolved lungs concentrations were measured by PET imaging after IV dosing of F18-pretomanid	[4]
Pyrazinamide	Pyrazinamide concentrations from blood plasma, lesions, and uninvolved lungs of mice after a single oral dose of 150 mg/kg pyrazinamide	[2]
Model Validation		
Bedaquiline	Bedaquiline and M2 concentrations from blood serum of pulmonary TB patients after bedaquiline doses ranging between 100 mg – 700 mg.	[5,6]
Pretomanid	Pretomanid serum concentrations from pulmonary TB patients after pretomanid doses ranging between 50 mg – 1200 mg.	[5,7,8]
Pyrazinamide	Pyrazinamide serum concentrations from pulmonary TB patients after 1500 mg daily dosing of pretomanid	[5]
Pyrazinamide	Pyrazinamide steady-state concentrations from lesions, and uninvolved lungs of pulmonary TB patients	[9]

S4.2. Final Model Codes for Bedaquiline and Pretomanid mPBPK.

```
BDQparams <- c(TVka1=1.3, TVka2=0.00501, TVCLint=60.3,
KpT=4.45, TVCLM2=45.9, KpTM2=18.4, Rles=11,
RUL=10.2, RlesM2=88.4, RULM2=88.8, TVfrc=0.609, fup=0.1 )
BDQmod <- RxODE({

################ Drug-specific Parameters Estimated and Translated to Humans
ka1=TVka1*exp(eta.ka1) ;
ka2 =TVka2*exp(eta.ka2) ;
CLint=TVCLint*((BW/70)^0.75)*exp(eta.CLint) ;
CLM2=TVCLM2*((BW/70)^0.75) *exp(eta.CLM2) ;
logit_frc = log(TVfrc/(1 - TVfrc)) ;

frc = (1 / (1 + exp(-logit_frc))) ;
################ Human System specific parameters ################
#Cardiac output
Qc = 312*(BW/70)^0.75 ; # Cardiac output (Brown 1997 table 22; calculated based on 5200 ml/min)
Qh = Qc*0.227 ; # Blood flow to liver as fraction of Qc (Brown1997 table 23)
Qt = Qc - Qh ;

# Volumes
VLiv = 0.0257*BW ; # Volume of liver (L) (Brown1997 table 7)
VLu = 0.0076*BW ; # Volume of lungs (L) (Brown1997 table 7)
Dblv = 0.0514 ; # Volume veins per kg BW (L/kg)
Dbla = 0.0257 ; # Volume arteries per kg BW (L/kg)
Dbl = Dblv + Dbla ; # Volume blood resovior per kg BW (L/kg)
Vbl = Dbl*BW ; # volume of blood resovioir (L)
Vt = BW - VLu - Vbl - VLiv ; # Residual body volume (L)

# Lesion volume calculation
# Median total lesion volume in cavitary TB patients = 14 mL (PMID: 34617068)
# 14 mL = 0.014 L represents ~2.16 % of total lung volume (total lung volume 0.532 L in 70 kg human)
# Assume comparable extent of lesions in Mtb infected mice
# VLeF = 0.014/0.53 ; # Volume of lung lesions (fraction of lung volume)
VULF = 1 - VLeF ; # Volume of lung lesions (fraction of lung volume)
VLe = VLeF*VLu ; # Absolute volume of lesion (L)
```

```
VUL = VLu - VLe ; # Volume of uninvolved lung (L)
QLe = Qc/VLe ; # Blood flow to lesion (1/hr)
QUL = Qc/VUL ; # Blood flow to uninvolved lungs (1/hr)

# Secondary parameters
Eh = (fup*CLint)/(Qh + (fup*CLint)) ;
Cbld = blood/Vbl ;
CbldM2 = M2blood/Vbl ;

################################## ODEs ################
d/dt(depot1) = -ka1*depot1 ; # Input
d/dt(depot2) = -ka2*depot2 ; # Input
d/dt(liver) = frc*ka1*depot1 + (1-frc)*ka2*depot2 - # Input
Qh*Eh*liver/VLiv - # conversion to M2
Qh*(1-Eh)*liver/VLiv + # outflow to blood
Qh*blood/Vbl ; # inflow from blood
d/dt(blood) = Qh*(1-Eh)*liver/VLiv - # absorption
Qh*blood/Vbl + # outflow to liver
tissue*Qt/(Vt*KpT) - blood*Qt/Vbl ; # in and out of tissues
d/dt(tissue) = blood*Qt/Vbl - tissue*Qt/(Vt*KpT) ;
d/dt(M2blood) = Qh*Eh*liver/VLiv - CLM2*M2blood/Vbl +
M2tissue*Qt/(Vt*KpTM2) - M2blood*Qt/Vbl ; # in and out of tissues
d/dt(M2tissue) = M2blood*Qt/Vbl - M2tissue*Qt/(Vt*KpTM2) ;
###Lesion and uninvolved lungs ODEs
d/dt(Cles) = QLe*(Cbld*Rles - Cles) ;
d/dt(CUlung) = QUL*(Cbld*RUL - CUlung) ;
d/dt(ClesM2) = QLe*(CbldM2*RlesM2 - ClesM2) ;
d/dt(CUlungM2) = QUL*(CbldM2*RULM2 - CUlungM2) ;

################ Outputs ################
C_plasma_bdq = (blood/Vbl)*1000 ; #ng/mL
C_liver_bdq = (liver/VLiv)*1000 ; #ng/mL ;
C_plasma_m2 = (M2blood/Vbl)*1000 ; #ng/mL ;
C_lesion_bdq = (Cles)*1000 ; #ng/mL ;
C_uninvolvedL_bdq = (CUlung)*1000 ; #ng/mL ;
C_lesion_m2 = (ClesM2)*1000 ; #ng/mL ;
C_uninvolvedL_m2 = (CUlungM2)*1000 ; #ng/mL ;
})
```

```
PTMparams <- c(
TVka=0.3,
TVCL=4.42,
TVED50=554,
TVKpT=36.24,
TVKpT1=0.48,
Rles=1.6,
RUL=1.76)

PTMmod <- RxODE({

################ Drug-specific Parameters Estimated and Translated to Humans #################
ka=TVka*exp(eta.ka) ;
CL=TVCL*exp(eta.CL)*(BW/70)^0.75 ;
KpT = TVKpT*exp(eta.KpT) ;
KpT1 = TVKpT1*exp(eta.KpT1) ;
ED50 = TVED50 ; #*exp(eta.ED50) ;
FT1 = 0.975 ;
BP = 1.65;

################ Human System specific parameters ################
#Cardiac output
Qc = 312*(BW/70)^0.75 ; # Cardiac output (Brown 1997 table 22; calculated based on 5200 ml/min)
Qt = Qc*(1 - FT1) ;
Qt1 = Qc*FT1 ;

# Volumes
VLu = 0.0076*BW ; # Volume of lungs (L) (Brown1997 table 7)
Dblv = 0.0514 ; # Volume veins per kg BW (L/kg)
Dbla = 0.0257 ; # Volume arteries per kg BW (L/kg)
Dbl = Dblv + Dbla ; # Volume blood resovior per kg BW (L/kg)
Vbl = Dbl*BW ; # volume of blood resovioir (L)
Vt_tot = BW - VLu - Vbl ; # Residual body volume (L)
Vt = Vt_tot*(1 - FT1) ;
Vt1 = Vt_tot*FT1 ;
```

```
# Lesion volume calculation
# Median total lesion volume in cavitary TB patients = 14 mL (PMID: 34617068)
# 14 mL = 0.014 L represents ~2.16 % of total lung volume (total lung volume 0.532
L in 70 kg human)
# Assume comparable extent of lesions in Mtb infected mice
# VLeF = 0.014/0.53 ; # Volume of lung lesions (fraction of lung volume)
VULF = 1 - VLeF ; # Volume of lung lesions (fraction of lung volume)
VLe = VLeF*VLu ; # Absolute volume of lesion (L)
VUL = VLu - VLe ; # Volume of uninvolved lung (L)
QLe = Qc/VLe ; # Blood flow to lesion (1/hr)
QUL = Qc/VUL ; # Blood flow to uninvolved lungs (1/hr)
Cbld = blood/Vbl ;

################################## ODEs #################
d/dt(depot) = -ka*depot ;
Fmax = 1 ;
doseIn = Fmax*dose/(1 + (dose/ED50)) ;
f(depot) = doseIn/dose ;
d/dt(blood) =ka*depot - CL*blood/Vbl + tissue*Qt/(Vt*KpT) - blood*Qt/Vbl +
tissue1*Qt1/(Vt1*KpT1) - blood*Qt1/Vbl ;
d/dt(tissue) = blood*Qt/Vbl - tissue*Qt/(Vt*KpT) ;
d/dt(tissue1) = blood*Qt1/Vbl - tissue1*Qt1/(Vt1*KpT1) ;
###Lesion and uninvolved lungs ODEs
d/dt(Cles) = QLe*(Cbld*Rles - Cles) ;
d/dt(CUlung) = QUL*(Cbld*RUL - CUlung) ;

################ Outputs #################
C_plasma = (Cbld/BP)*1000 ; #ng/mL
C_lesion = (Cles)*1000 ; #ng/mL
C_Ulung = (CUlung)*1000 ; #ng/mL})
```

S4.3. Pyrazinamide mPBPK model in mice. (A) Model structure, (B) Model fit. blue points=observed data, black line=model fit predictions.

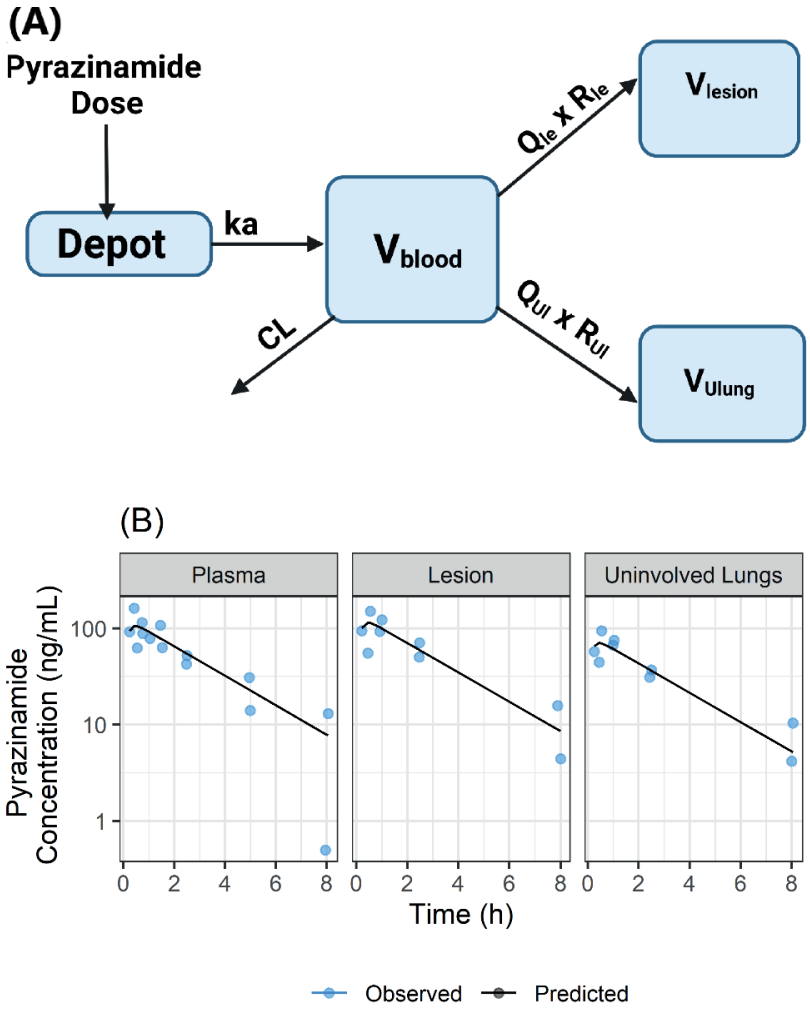

S4.4. Time course of Bedaquiline Metabolite, M2, concentrations, (A) Plasma, lungs, and lesion observed vs. model predictions in mice, (B) Plasma in TB patients. The model predictions for bedaquiline well with the observed data for mice and TB patients from clinical trials at clinically-relevant doses. Bedaquiline was administered orally as 25 mg/kg in mice and 400 mg on day1, 300 mg on day2, and 100 mg QD on day3 onwards in patients[5]. Red horizontal line refers to half-maximal M2 concentrations for QTcF prolongation[10].

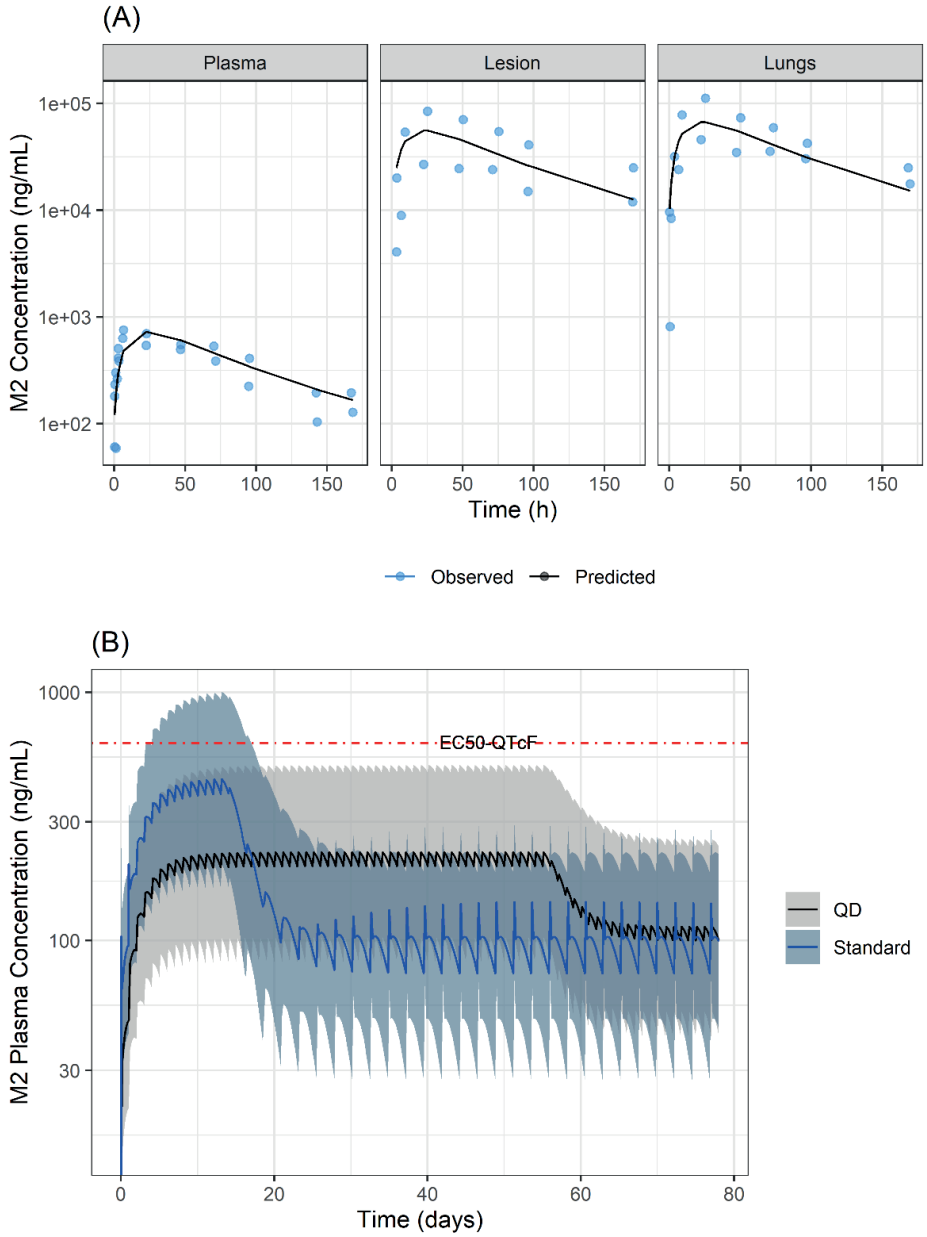

S4.5. Predicted and observed plasma steady-states PK pProfiles in TB patients for Bedaquiline, M2, and Pretomanid. Blue points=observed data, solid grey line=median of the simulations, shaded grey area=95% confidence interval (CI) of the simulations. Panel titles represent bedaquiline or pretomanid doses in mg. Bedaquiline was administered as an increasing daily dose, i.e., panel 1 represents a group that received 200 mg on day1 and 100 mg on day2 onwards.

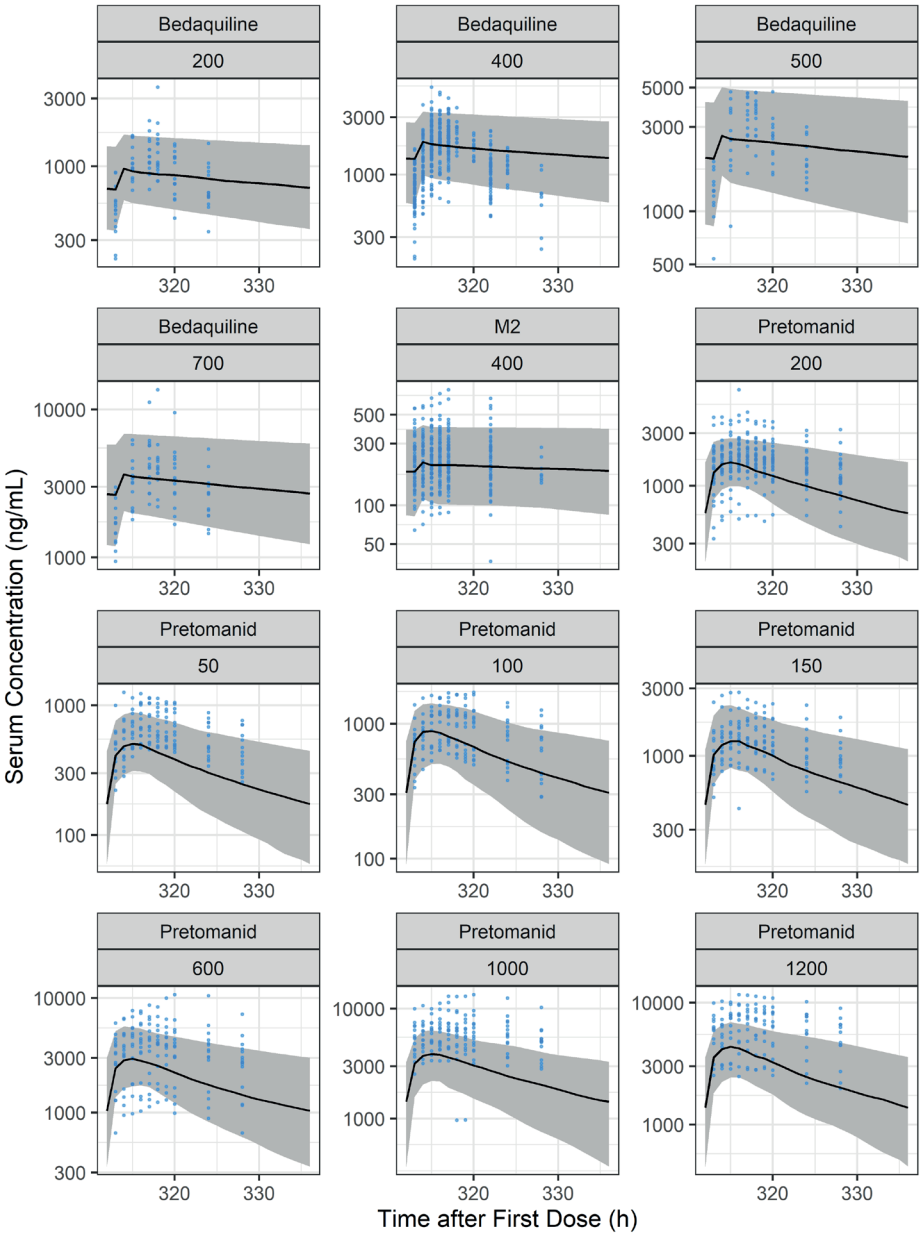

S4.6. Local sensitivity Analysis. The sensitivity of the parameter estimates on steady-state plasma drug exposure was examined by introducing 10% or 50% variation in the parameters one at a time and running the simulations for 50 times. Overall, the mean sensitivity index was low (between -2.5 and 2.5) for both bedaquiline and pretomanid with the exception of ka2 of bedaquiline that showed high sensitivity to affect both bedaquiline and M2 plasma concentrations, and kpT1 showed relatively moderate sensitivity to affect pretomanid plasma concentrations. Points and error bars represent mean (95% CI) of the sensitivity index.

10%

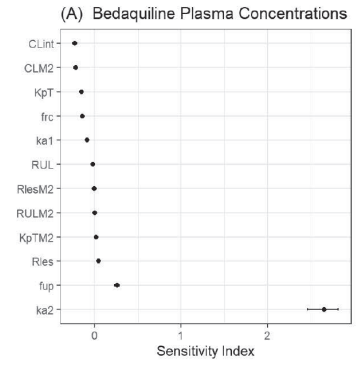

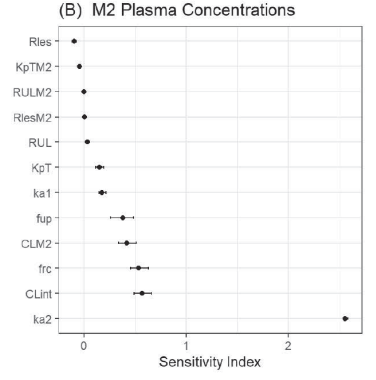

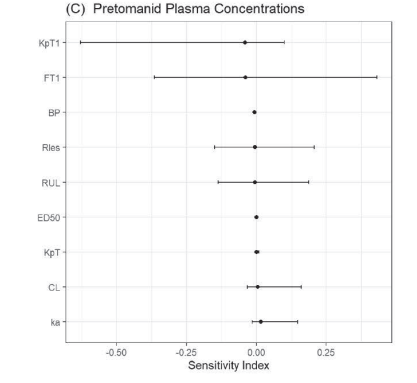

50%

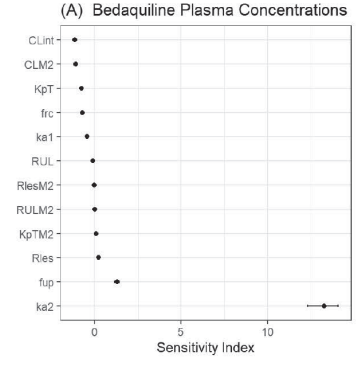

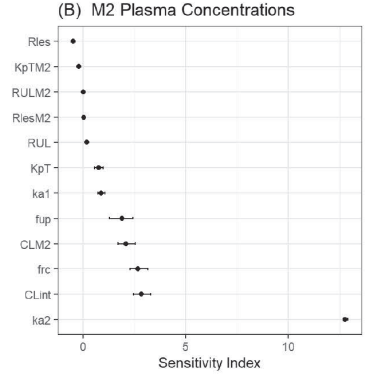

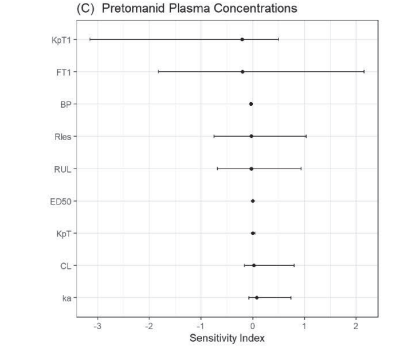

References

1. Rouan MC, Lounis N, Gevers T, Dillen L, Gilissen R, Raoof A, et al. Pharmacokinetics and pharmacodynamics of TMC207 and its N-desmethyl metabolite in a murine model of tuberculosis. Antimicrob Agents Chemother. 2012;56(3):1444–51.
2. Irwin SM, Prideaux B, Lyon ER, Zimmerman MD, Brooks EJ, Schrupp CA, et al. Bedaquiline and Pyrazinamide Treatment Responses Are Affected by Pulmonary Lesion Heterogeneity in Mycobacterium tuberculosis Infected C3HeB/FeJ Mice. ACS Infect Dis. 2016;2(4):251–67.
3. Ahmad Z, Peloquin CA, Singh RP, Derendorf H, Tyagi S, Ginsberg A, et al. PA-824 exhibits time-dependent activity in a murine model of tuberculosis. Antimicrob Agents Chemother. 2011;55(1):239–45.
4. Mota F, Ruiz-Bedoya C, Tucker E, De Jesus P, Flavahan K, Turner M E, C, Bahr M, Kim J, Farina M, Peloquin CA, Ordonez A JS. Noninvasive Assessment of Intralesional Antimicrobial Concentration- Time Profiles in Pulmonary and Central Nervous System Tuberculosis using Dynamic 18F-Pretomanid Positron Emission Tomography. OFID 20218 Sess P-80 Tuberc other Mycobact Infect. 2021;789–90.
5. Diacon AH, Dawson R, Von Groote-Bidlingmaier F, Symons G, Venter A, Donald PR, et al. Bactericidal activity of pyrazinamide and clofazimine alone and in combinations with pretomanid and bedaquiline. Am J Respir Crit Care Med. 2015;191(8):943–53.
6. The global alliance for tb drug development. Evaluation of Early Bactericidal Activity in Pulmonary Tuberculosis (TMC207-CL001). https://clinicaltrials.gov/show/NCT01215110. 2017.
7. Diacon AH, Dawson R, Du Bois J, Narunsky K, Venter A, Donald PR, et al. Phase II dose-ranging trial of the early bactericidal activity of PA-824. Antimicrob Agents Chemother. 2012;56(6):3027–31.
8. Dawson R, Diacon AH, Everitt D, van Niekerk C, Donald PR, Burger DA, et al. Efficiency and safety of the combination of moxifloxacin, pretomanid (PA-824), and pyrazinamide during the first 8 weeks of antituberculosis treatment: a phase 2b, open-label, partly randomised trial in patients with drug-susceptible or drug-resistant pul. Lancet [Internet]. 2015 May 2;385(9979):1738–47. Available from: https://doi.org/10.1016/S0140-6736(14)62002-X
9. Prideaux B, Via LE, Zimmerman MD, Eum S, Sarathy J, O'Brien P, et al. The association between sterilizing activity and drug distribution into tuberculosis lesions. Nat Med. 2015;21(10):1223–7.
10. Tanneau L, Karlsson MO, Rosenkranz SL, Cramer YS, Shenje J, Upton CM, et al. Assessing Prolongation of the Corrected QT Interval with Bedaquiline and Delamanid Coadministration to Predict the Cardiac Safety of Simplified Dosing Regimens. Clin Pharmacol Ther. 2022;0(0):1–9.